IEEE Access
Multidisciplinary | Rapid Review | Open Access Journal

Received November 12, 2017, accepted December 21, 2017, date of publication January 4, 2018, date of current version March 9, 2018.

Digital Object Identifier 10.1109/ACCESS.2017.2789216

Development of Efficient High Power Amplifier With More Than an Octave Bandwidth

WAQAR AHMAD MALIK, ABDELFATTAH AHMAD SHETA, AND IBRAHIM ELSHAFIEY
Department of Electrical Engineering, King Saud University, Riyadh 11421, Saudi Arabia

Corresponding author: Waqar Ahmad Malik (wmalik@ksu.edu.sa)

This work was supported by the University Research Program of King Abdulaziz City for Science and Technology and Lockheed Martin Corporation.

ABSTRACT This paper presents a design of a GaN HEMT-based power amplifier (PA), with enhanced efficiency and linearity over the operation band from 0.5 to 1.5 GHz. The design is based on wideband load-pull and source-pull analysis. A novel procedure is developed to optimize the impedance values and synthesize the matching networks. The amplifier achieves drain efficiency of 40%–68% and power added efficiency (PAE) of 35.7%–63.8%, over the entire frequency band measured for an input power of 24 dBm. To ensure flat gain response, a high pass filter is deployed at the input of the PA, thus achieving a gain of 13.8 ±1 dB for the entire band. Wideband matching circuits are realized on Taconic RF35 with dielectric constant of 3.5 and thickness of 0.76 mm. The PA is found to maintain output power of 36.8–38.3 dBm across the frequency band. Carrier to intermodulation distortion ratio for two-tone input signal with 24-dBm power per-tone and a spacing of 5 MHz is found to be better than 30 dB. In addition, the PA is tested for frequency spacing values of 20 and 25 MHz and good linearity levels are attained. The developed PA thus provides attractive features related to efficiency, linearity, and extended bandwidth, which make this amplifier appropriate for implementations in various wireless communications systems.

INDEX TERMS GaN HEMT, high efficiency, power added efficiency (PAE), wideband high power amplifier.

I. INTRODUCTION

The rapid progress in wireless communication systems necessitates the development of wireless nodes that can achieve the operation according to various technology standards. Wideband components are required to design such nodes. In particular, the characteristics of the PA have great impact on the overall bandwidth, energy consumption, and efficiency of the entire RF system. Wideband power amplifier designs are in great demand to allow operation at various frequency bands.

Broadband power amplifier is typically achieved by adopting the distributed topology. Distributed PA designs provide excellent bandwidth enhancements but they lack the ability to provide high efficiency. The efficiency achieved by distributed PA topology is normally in range of 20-30% [5]. In addition, the distributed PA arrangement has high complexity due to the existence of more than one FET. Therefore, a high efficiency and linearized PA along with the broadband capability is strongly recommended for next generations of wireless communication systems. High linearity helps to serve the high peak to average power ratio (PAPR) requirement of existing communication systems. However, the high efficiency PA can meet the stringent low power consumption requirement of the upcoming as well as existing wireless generation standards.

Moreover, proper transistor selection is essential in implementing high power amplifier. Emerging technologies of Gallium Nitride high electron mobility transistor (GaN HEMT) are attractive for enhanced PA performance, due to the associated features of high breakdown voltage, high power density and high electron mobility [6]. Due to these profound advantages, GaN HEMT have been the target of design of various broadband high power amplifiers as reported in [7]–[9].

Several broadband 10 Watts Cree's GaN HEMT (CGH40010) based PAs were reported as summurized in Table I. A 2-3.5 GHz broadband GaN HEMT PA reported in [1], which achieves a PAE of 64-76% and 40 dBm of output power at an input power drive of 30 dBm. The attained gain is 13 dB for the reported frequency band. The design is based on loadpull analysis, while a low pass broadband

TABLE 1. State of the art 10 Watts (CGH4001F) GaN HEMT based wideband power amplifiers.

Ref	Pout (dBm)	Drain Efficiency (%)	Bandwidth GHz, (%)	Gain (dB)	Input power drive (dBm)
[1], 2014	40	64-76	2-3.5, (54.5)	13	30 dBm
[2], 2014	>39.3	>56.8	1-2.9, (97)	>10.3	29 dBm
[3], 2016	41	68	1.4-2.7, (63.4)	9	31 dBm
[4], 2013	36-38.5	45-60*	1.6-2.6, (47.6)	14.2-15.6	--
This Work	36.8-38.3	40-68	0.5-1.5, (100)	12.8-15.2	24 dBm

* PAE

stepped impedance matching network is utilized to achieve the optimum impedances. Another design [2] is concerned with 1-2.9 GHz, 10 watts GaN HEMT based PA. The design is based on continuous mode to offer broadband characteristics and achieve PAE greater than 60% along for continuous wave power of >8.5 W at an input power level of 29 dBm. In [3], a Class E PA with shunt capacitance and shunt filter is reported. Reactance compensation technique is used to enhance the broadband capability of the proposed PA. The amplifier achieves an average drain efficiency of 68% and 41 dBm of output power at a high input power level of 31 dBm. However, a gain of only 9 dB across a band of 1.4-2.7 GHz is realized. A broadband PA biased in deep Class AB mode with drain current of 35 mA is presented in [4]. The design is based on harmonic control technique and achieves a power-added-efficiency (PAE) of 45-60%, along with 36-38.5 dBm output power, for a coverage band of 1.6-2.6 GHz (i.e. bandwidth of 47.6%).

In this work, we propose the design of a wideband high power amplifier centered at 1 GHz with a high fractional bandwidth of 100%. The PAE for the entire band (i.e. 500 MHz to 1.5 GHz) is 35.7-63.8%, while the drain efficiency is 40-68% at 24 dBm input power level. Almost a flat gain of 12.8-15.2 dB is obtained for the whole band. Moreover, a maximum output power of 38.3 dBm is achieved. The proposed PA archives the highest fractional bandwidth in comparison to designs presented in Table 1, and thus is suitable for recent and future wireless communication systems. Furthermore, the Output power and efficiency are measured at 1 dB compression point, rather deep in saturation (i.e. input power >24 dBm).

This article is organized as follows. Section II presents the step-by-step design procedure of the PA: firstly, the selection of compromised optimum impedances. Secondly, the matching networks synthesis design steps, and finally the small signal analysis and optimization of the overall PA along with the preservation of flat gain over the desired bandwidth. Section III presents the large-signal analysis with the PA excited with 1-tone and 2-tone input signals and their results in terms of PAE, Pout, Gain, and linearity as well.

TABLE 2. Optimum load & source impedances.

Frequency	Source Impedance (Ω)	Load Impedance (Ω)
500 MHz	20+j16	51+j15
1000 MHz	8+j9	41+j28
1500 MHz	7 + j0	28+ j29

II. POWER AMPLIFIER DESIGN

The device selected for the design is 10 watts GaN HEMT (CGH40010P), with a broadband operation of up to 6 GHz, that is best suited for the design of broadband amplifiers [10]. The non-linear model of the device, provided by the manufacturer is utilized for simulations performed in RF & Microwave CAD Advanced Design System (ADS).

Since the harmonics of the desired fundamental frequencies fall inside the desired bandwidth, harmonic tuning techniques like Class E, Class F and others cannot be adopted here [11]. Consequently, the FET is biased as Class AB, due to its well-adjusted performance in both linearity and efficiency. The gate to source voltage of '$V_{gs} = -2.5$ Volts' & Drain to source voltage of '$V_{ds} = 28$ Volts' are applied at the gate and drain respectively, resulting in a drain quiescent current of 200 mA. To stabilize the transistor, a stability network comprising of two parallel RC pair of '4.7 pF & 27 ohms and 18 pF and 22 ohms' are cascaded in series fashion. After proper biasing and stabilization of the transistor, the input and output matching networks are designed for enhancing efficiency, gain and output power. In order to find the optimum impedances at the input and output of the GaN HEMT, loadpull analysis simulation are performed.

A. LOAD-PULL ANALYSIS AND OPTIMUM IMPEDANCES SELECTION

The optimum source and load impedance values are found to be very close to those provided in [10]. Optimum source and load impedance values are the basis of realizing input and output matching circuits, which is the most challenging step in the design of the PA. Table 2, shows the optimum source and load impedances at discrete frequencies of 0.5, 1, & 1.5 GHz with respect to $V_{DS} = 28$ V, and $I_{DS} = 200$ mA [10].

Likewise, the loadpull analysis are performed at input power equal to 1 dB gain compression (i.e. $P1_{dB} = 24$ dBm), Vds = 28 Volts, and Vgs = −2.5 Volts, resulting in constant output power and PAE contours for different load impedances. The PAE and output power (Pout) contours are plotted on smith charts for different frequencies as shown in Fig. 1(a). The three different plots in Fig. 1(a) shows the PAE and Pout contours for 0.5 GHz, 1 GHz, & 1.5 GHz with respect to load impedances. As noticed, the impedance variation with respect to the frequency, as expected, demonstrates a shift in the contours plotted for the load impedances. This necessitate the selection of a conceded optimum impedance

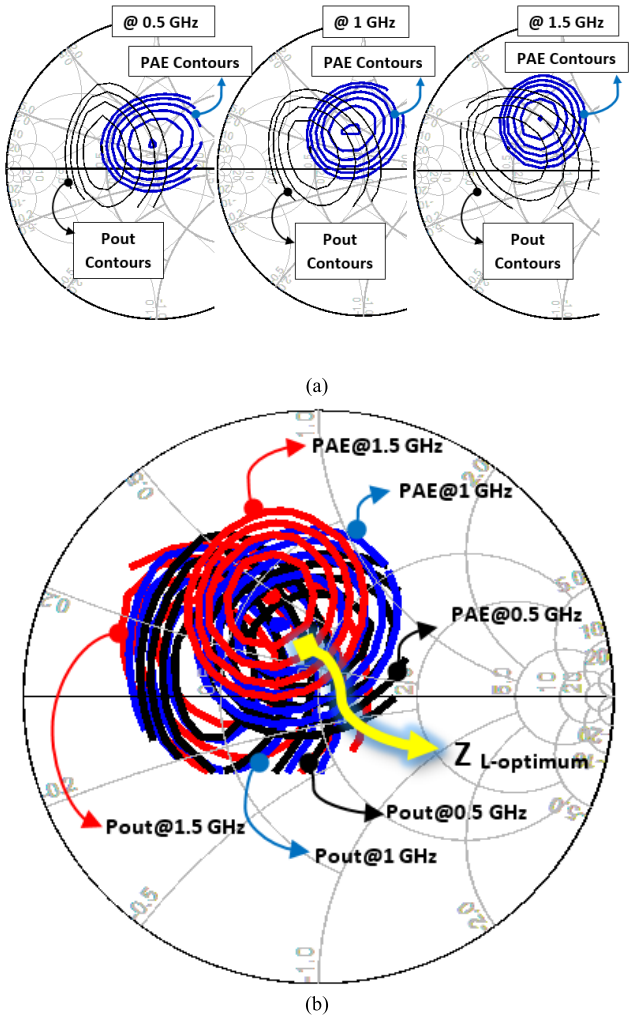

FIGURE 1. (a) PAE and output power contours for 0.5 GHz (left), 1 GHz (middle) & 1.5 GHz (right) with respect to load impedances (b) Compromised $Z_{L\text{-optimum}}$ selected on combined PAE and output power contours plot for all frequency points.

that accommodates high efficiency, gain, and high output power simultaneously. This can be accomplished by merging all the contours of Fig. 1(a) on a single smith chart. Thus, Fig. 1 (b) shows the combined PAE and output power (P_{out}) contours on single Smith Chart for all frequencies. Hence, the compromised optimum load impedance "$Z_{L\text{-optimum}}$" is selected to be 31+j7 ohms at center frequency i.e. 1 GHz as shown in Fig. 1. Similarly, the compromised source impedance "$Z_{S\text{-optimum}}$" is selected in the same way and turns out to be 14+j18 Ohms. The selected impedances demonstrate good performance for the desired frequency band in terms of PAE, and output power. Table 3 shows the resulting figure merits of the selected conceded $Z_{L\text{-optimum}}$ and $Z_{S\text{-optimum}}$. This is the starting point for the design of the wideband matching circuits bearing high performance to deliver the desired PAE and output power, however, a slight degradation in performance is expected due to experimental losses.

TABLE 3. PAE and output power for selected compromised load impedance.

Frequency	PAE (%)	Output Power (dBm)
500 MHz	69	42.3
1000 MHz	67	42.1
1500 MHz	60.5	40.8

B. STEP BY STEP DESIGN OF WIDEBAND MATCHING NETWORKS

Wideband matching networks required at both ends of the FET shall comply with the impedance transformation of *1:* $Z_{S-Optimum}$ and $Z_{L-Optimum}$*:1* at input and output respectively. The design of the matching networks is based on 0.5 dB equal-ripple low-pass prototype filter and takes the following steps;

Step 1 (Low-Pass Prototype Extraction): A third-order normalized low-pass prototype values are extracted from [12] as shown in Fig. 2(a).

Step 2 (Richard's Transformation): Richard's transformation [13], is used to convert the shunt capacitors to shunt stubs and series inductors to series stub. The characteristic impedance 'Z_0' of a shunt stub is '1/C' with a length of $\lambda/8$ at $\omega = 1$ rad/sec according to (1), while the series inductor's $Z_0 = L$ with a length of length of $\lambda/8$ at $\omega = 1$ rad/sec according to (2).

$$jB_C = j\Omega C = jC\tan\beta l \Rightarrow Z_0 = 0.911 \quad (1)$$

$$jX_L = j\Omega L = jL\tan\beta l \Rightarrow Z_0 = 1.596 \quad (2)$$

The transformation maps the ω plane to Ω plane, where, $\Omega = tan\beta l$. However, all the commensurate synthesized lines are $\lambda/8$ long at $\omega = \omega_c$ as shown in Fig.2 (b).

Step 3 (Kuroda Transformation): Since the series stubs cannot be realized using microstrip lines, therefore one of the Kuroda identity [14] is used to convert them into shunt stubs. The transformation factor n^2 (3) is used to acquire the characteristic impedances of the transformed shunt stubs as shown in Fig. 2 (c).

$$n^2 = 1 + \frac{Z_{02}}{Z_{01}} = 1.626 \quad (3)$$

Step 4 (Impedance and Frequency Scaling): The impedance scaling is done by simply multiplying the normalized impedances with 50 ohms and transforming the lengths of the shunt stubs to $\lambda/8$ at 1.5 GHz. The resulting circuit is shown in Fig. 2 (d).

Step 5 (Complex-to-Real Transformation): The real-to-real network is first scaled from 50 ohms to our desired 31 ohms and then transformed to complex-to-real using ADS optimizer. The DC block capacitor of 100 pF and $\lambda/4$ length line for Drain bias are fixed to end up with a final output matching network. Although, the optimization is still required once the designed network is integrated with the FET to help us improve the PAE, output power and gain. The final

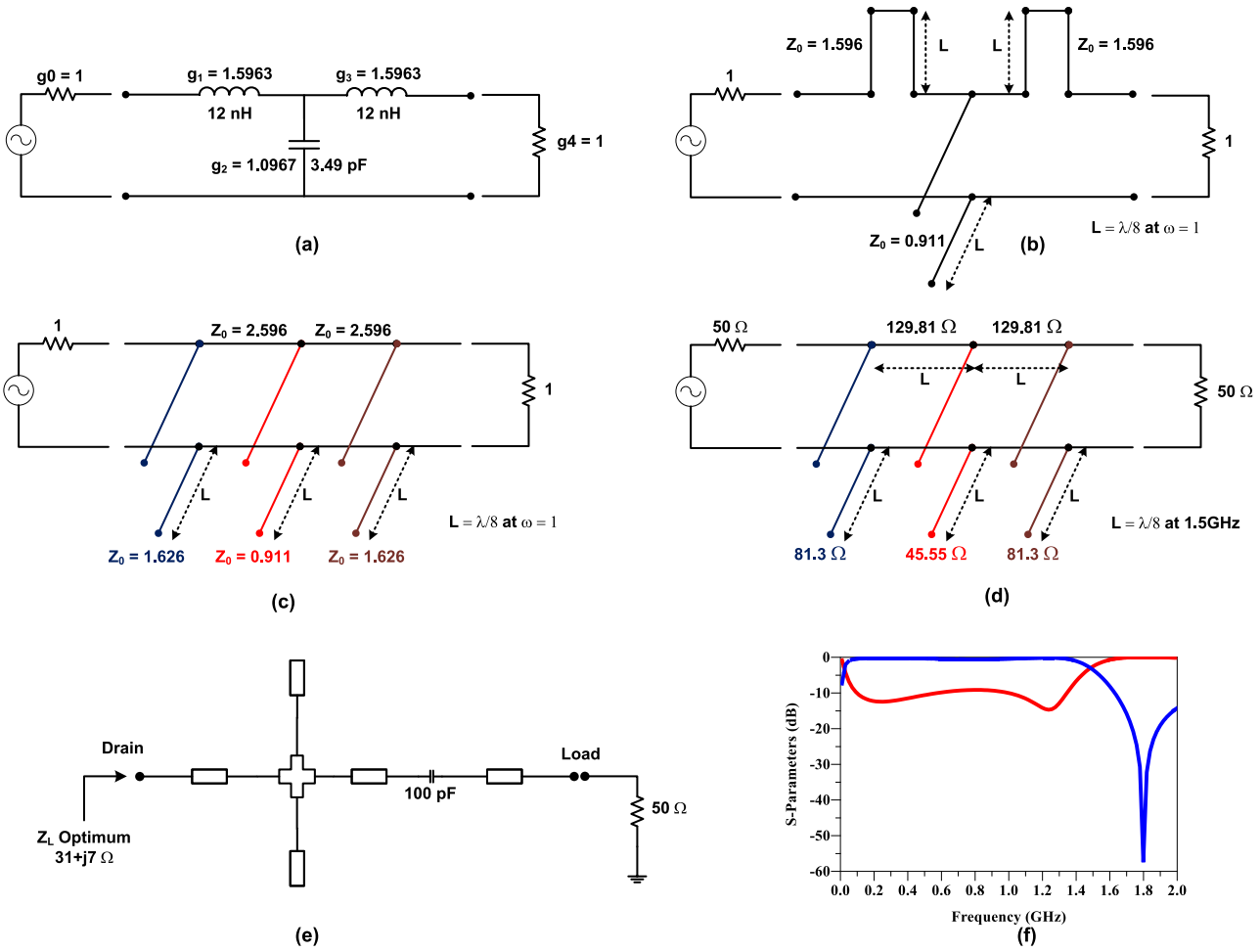

FIGURE 2. Steps in designing the wideband output matching circuit: (a) 0.5 dB Equal-Ripple Low pass filter prototype with N = 3. (b) Richard's transformation to convert series inductor to series stub and shunt capacitor to shunt stub. (c) using Kuroda's identity to convert the series stub into a shunt stub. (d) Impedance scaling. (e) Complex-to-real optimized microstrip output matching network derived from the circuit in 'e' (f) S_{11} (dB)-(red) & S_{21} (dB)-(blue) response of the optimized matching network.

optimized realizable distributed output matching network is shown in Fig 2 (e), while Fig. 2 (f), shows its return loss and gain response.

Similarly, the input matching network is also synthesized is similar fashion to end up with an input matching network, shown in Fig. 3 (a). The s-parameters plot for the overall PA is shown in Fig. 3 (b). It is noticed that the transducer power gain is bizarrely high at low frequencies (emphasized with circle in Fig 3(b)) and thus, contributing to a non-flat response. Subsequently, an optimization is required to achieve a flat gain over the entire band of interest.

C. MAINTAINING THE GAIN FLATNESS IN THE ENTIRE BAND

It is highly desirable for a wideband high power amplifier to have a flat gain response for the entire band of frequencies. To achieve this, a high pass filter with cutoff frequency of around 400 MHz and a ripple value of not more than 0.2 dB in the passband can be used to maintain the overall response of the input matching circuit. For this, the proposed microstrip high pass filter (HPF) is designed. The HPF and its response is shown in Fig. 4, and thus appears to be suitable to be incorporated in the matching network. Fig. 7 shows the proposed PA's schematic with the designed filter been integrated in the input matching network. While, the Simulated S-parameters response of the PA with and without the high pass filter is shown in Fig. 5. It is clearly evident from the response that beyond 600 MHz the gain is not altered much after integration of the filter, however, the response at low frequency is highly improved, resulting in almost flat gain response for the entire band. This effect can easily be realized in measured S-parameters response shown in Fig. 6.

III. LARGE SIGNAL ANALYSIS

The fabricated PA circuit base is tacked with a 2 mm aluminum plate using conductive epoxy. The aluminum plate is properly engraved for the placement of the device and hence acts as a heat sink. The resistors, capacitors, and SMA connectors are soldered before the placement of the FET. Fig. 8 shows the photograph of the fabricated PA.

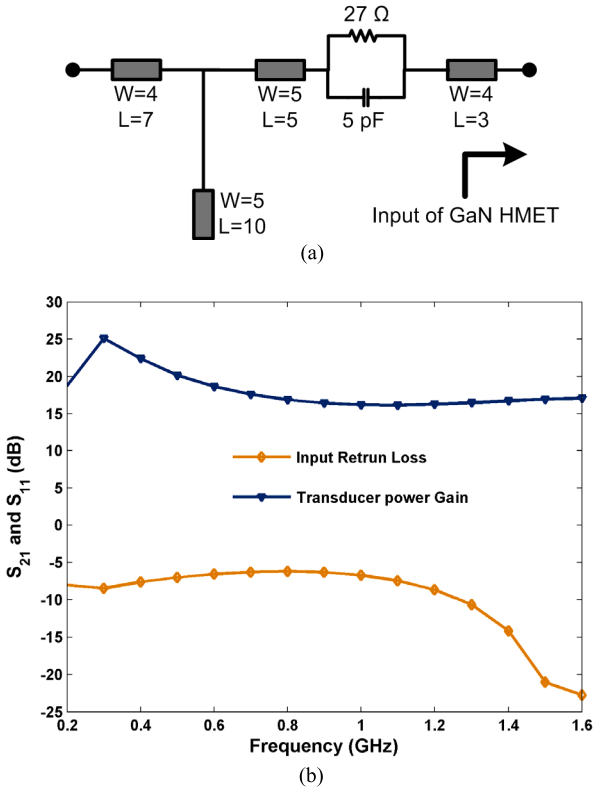

FIGURE 3. (a) Optimized Input Matching Network and (b) its response S_{11}, S_{21} (dB) versus Frequency (GHz), after initial optimization.

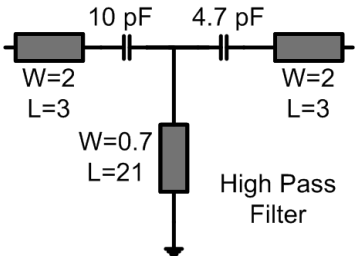

FIGURE 4. Proposed High Pass Filter.

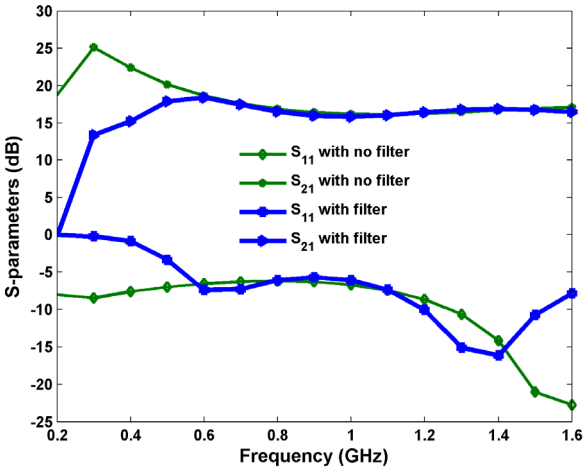

FIGURE 5. Comparison in performance of PA with and without HPF, Simulated S-parameters (dB) versus Frequency (GHz).

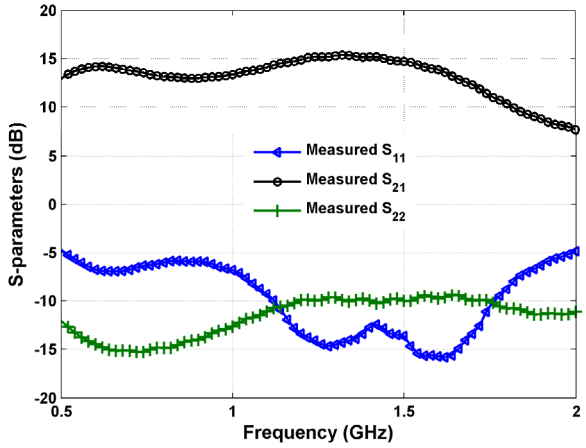

FIGURE 6. Measured S-parameters (dB) over the entire frequency band (GHz).

A. 1-TONE MEASUREMENTS

The PAE, gain and output power measurements are done when the PA is excited with 1-tone signal. Fig 9 shows the 1-tone measurement setup with Hittite HMC-T2100 signal generator, GW-Instek SPD-3606 dual range DC power supply, 50 Watts Aeroflex 20 dB attenuator, directional coupler (Agilent-83700B), 5 Watts 20 dB attenuator, 50 ohms' termination, and Anritsu MS2717B. As per standard procedure of the measurement the dual DC power supply is used to bias the gate and drain with negative and positive DC voltage respectively. The channel of the GaN HMET is first closed by applying -5V at the Gate-Source junction, thus allowing us to safely apply the 28V at the drain-source junction. Once the drain-source voltage is applied, the gate-source voltage is increased to a level to allow 200 mA of drain current approximately. This allows us to now apply RF signal at input and record measurements at the output of the PA. Fig. 10 shows the measured PAE, output power, and gain over the band of 0.5-1.5 GHz. The measured PAE is 35.7-63.8 %, while maximum output power of 38.3 dBm, and gain of 12.8-15.2 dB is recorded for 24 dBm of input power. Due to some experimental setup limitations an incremental change in length of lines is done that slightly reduced the performance of the power amplifier. Figure 11, shows the power added efficiency for different discrete frequencies i.e. 0.5 GHz, 0.8 GHz, 1.4 GHz, & 1.5 GHz with respect to the input power (dBm). Likewise, the Input-Output power characteristics at different discrete frequencies (i.e. 0.5 GHz, 0.8 GHz, 1.4 GHz, & 1.5 GHz) is presented in Figure 12.

B. LINEARITY CHARACTERISTICS BY APPLYING TWO-TONE SIGNAL

The most commonly method to measure the linearity metrics is to excite the PA with two-tone signal of same power and observe the two amplified signal along with its

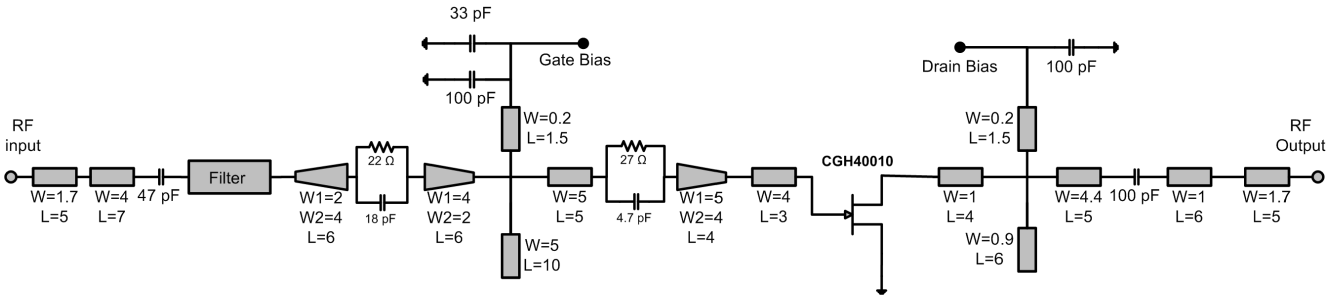

FIGURE 7. Final Schematic of the proposed wideband Power Amplifier.

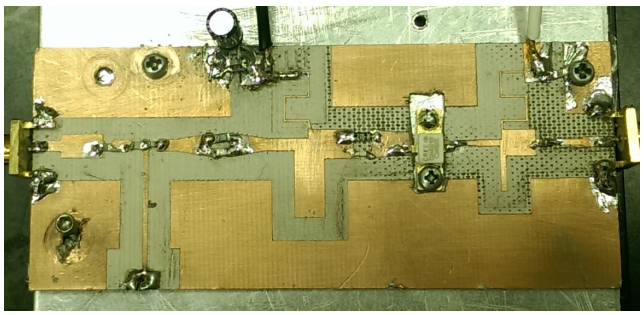

FIGURE 8. Photograph of the fabricated wideband high power amplifier.

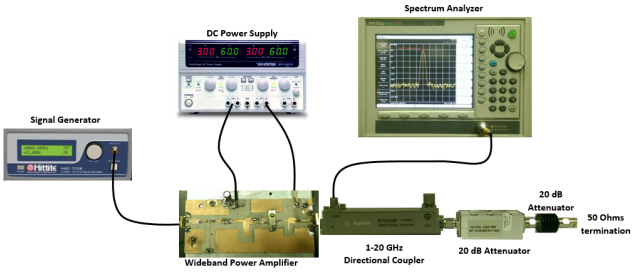

FIGURE 9. 1-tone PAE, Pout & Gain measurement setup.

TABLE 4. Linearity analysis for different values of Vgs.

Gate-to-source Voltage (V)	C/IMD3$_{LEFT}$ (dB)	C/IMD3$_{RIGHT}$ (dB)
-3	19.3	18.5
-2.8	23.7	23.2
-2.5	**27**	**30**
-2.3	23.2	25.1
-2	21.6	22.6

intermodulation distortions (IMDs). The difference between the carrier and 3rd order IMD (IMD3) exhibits the linearity of the PA. The IMD3s are not symmetric for even the same input power of both tones [15], and are thus calculated as shown in (4) and (5).

Due to the selection of Class AB operation, a good linearity is expected at the output. To validate the concept, the input power of both the tones is fixed and the 3rd order IMDs

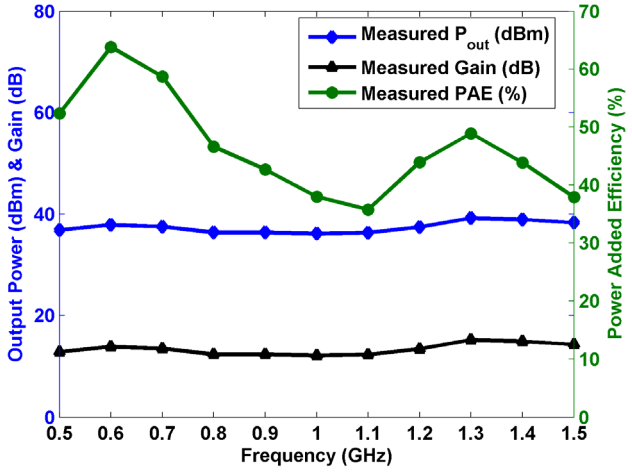

FIGURE 10. Measured PAE (%), Output Power (dBm) and Gain (dB) over the entire frequency band with Input Power of 24 dBm.

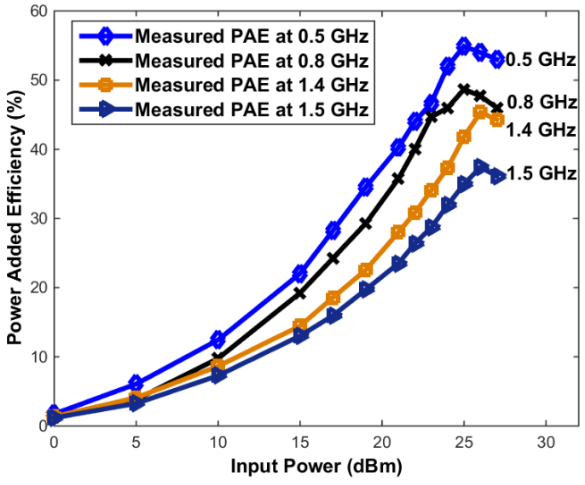

FIGURE 11. Measured Power Added Efficiency 'PAE' (%) with respect to input power sweep (dBm) for 0.5, 0.8, 1.4, & 1.5 GHz.

are observed for different values of Vgs. Table 4, shows the linearity metrics for different Vgs values for −2 V, −2.3 V, −2.5 V, −2.8V, and −3 V. Hence, Vgs = −2.5 V proves to be the best value for biasing the PA to provide good linearity.

$$C/IMD3_{LEFT} = P_{OUT-f1} - P_{OUT-2f1-f2}(dB) \quad (4)$$

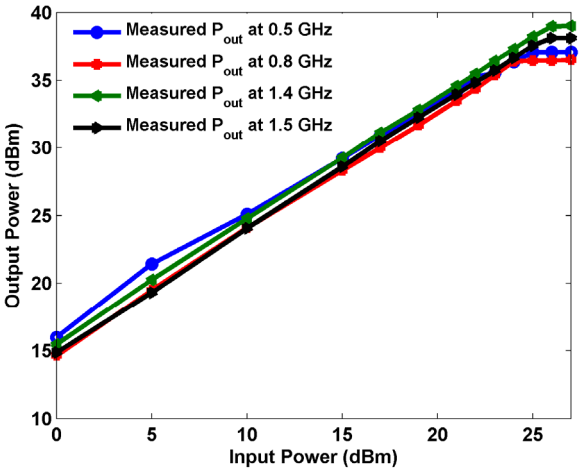

FIGURE 12. Measured Output power (dBm) vs. Input Power sweep (dBm) for 0.5, 0.8, 1.4, & 1.5 GHz.

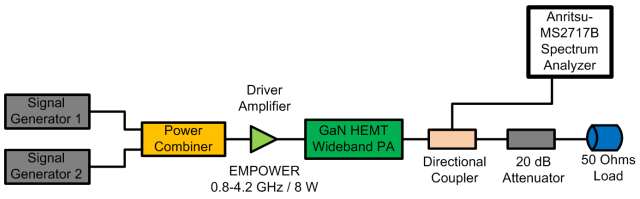

FIGURE 13. Two-tone measurement setup with 24 dBm input power for each tone.

TABLE 5. Linearity analysis for different carrier frequencies and spacing of 5 MHz.

Carrier Frequency (MHz)	$C/IMD3_{LEFT}$ (dB)	$C/IMD3_{RIGHT}$ (dB)
f_1= 800 MHz f_2= 805 MHz	30.2	27.3
f_1= 1000 MHz f_2= 1005 MHz	29.14	29.5
f_1= 1100 MHz f_2= 1105 MHz	27.2	30.4

TABLE 6. Linearity analysis for different spacing between F_1 and F_2.

Δf (f_2-f_1)	$C/IMD3_{LEFT}$ (dB)	$C/IMD3_{RIGHT}$ (dB)
5 MHz	30.8	30.2
20 MHz	20.2	23.5
25 MHz	23	27.3

$$C/IMD3_{RIGHT} = P_{OUT-f2} - P_{OUT-2f2-f1}(dB) \quad (5)$$

The two-tone measurement setup includes two signal generators producing two-tones with same power level (i.e. 24 dBm) and then combining them using power combiner. The two-tones are then amplified using EMPOWER's (SKU-1030) 800-4200 MHz driver amplifier and then fed to our proposed GaN HEMT wideband PA, as shown in Fig 13. The two-tone analysis is carried out at 1 dB compression point that is 24 dBm for each tone. The measurements are performed for two-tones with different carrier frequencies while

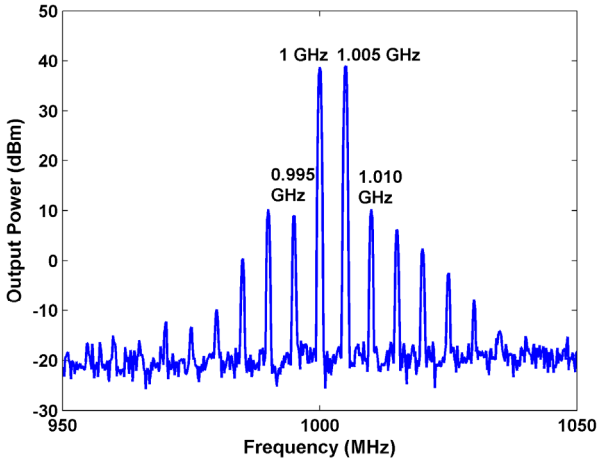

FIGURE 14. Measured Output Spectrum for two-tone input signal with 24 dBm power per-tone and spacing of 5 MHz.

maintaining the spacing of 5 MHz as expressed in Table 5. Fig. 14 shows the output spectrum of the PA excited with two-tone input signal at 1 GHz (f_1) and 1.005 GHz with spacing of 5 MHz (f_2-f_1). In next step, the two-tone measurements are done with 24 dBm 2-tone input signal along with different spacing between f_1 and f_2 i.e. $\Delta f = 5$MHz, 20 MHz, 25 MHz. The carrier to intermodulation distortion ratio for each spacing is shown in Table 6, demonstrating good linearity measure at 1-dB compression point.

IV. CONCLUSION

A wideband high power amplifier based on GaN HEMT is proposed in this work. The proposed PA achieves a drain efficiency of 40-68 % for a more than one octave bandwidth (0.5-1.5 GHz), thus offering a high fractional bandwidth of 100%. Furthermore, a step-by-step procedure of extracting the compromised optimum impedance from the wideband loadpull analysis is presented. The required optimum impedances are realized by synthesizing the low-pass filter prototype to the final distributed matching network. The matching network synthesis steps are elaborated. Furthermore, a flat gain response is achieved by incorporating a high-pass filter in the input matching network. The output power of almost 39 dBm is achieved for the desired operating band.

For the linearity analysis the PA is tested with a two-tone 24 dBm input signal with different frequency spacing of 5 MHz, 20 MHz, & 25 MHz. The C/IMD3 of 30.8 dB is observed at 1-dB compression point. The overall performance and specifically broadband characteristic of the proposed PA makes it attractive for utilization in next generation wireless communication systems.

REFERENCES

[1] J. Xia, X.-W. Zhu, and L. Zhang, "A linearized 2–3.5 GHz highly efficient harmonic-tuned power amplifier exploiting stepped-impedance filtering matching network," *IEEE Microw. Wireless Compon. Lett.*, vol. 24, no. 9, pp. 602–604, Sep. 2014.

[2] T. Canning, P. J. Tasker, and S. C. Cripps, "Continuous mode power amplifier design using harmonic clipping contours: Theory and practice," *IEEE Trans. Microw. Theory Techn.*, vol. 62, no. 1, pp. 100–110, Jan. 2014.

[3] A. Grebennikov, "High-efficiency class-E power amplifier with shunt capacitance and shunt filter," *IEEE Trans. Circuits Syst. I, Reg. Papers*, vol. 63, no. 1, pp. 12–22, Jan. 2016.
[4] C. Huang, S. He, F. You, and Z. Hu, "Design of broadband linear and efficient power amplifier for long-term evolution applications," *IEEE Microw. Wireless Compon. Lett.*, vol. 23, no. 12, pp. 653–655, Dec. 2013.
[5] N. Kumar and A. Grebennikov, *Distributed Power Amplifiers for RF and Microwave Communications*, Norwood, MA, USA: Artech House, 2015.
[6] A. Kistchinsky, *Ultra-Wideband GaN Power Amplifiers-From Innovative Technology to Standart Products*. Rijeka, Croatia: InTech, 2011.
[7] O. Kizilbey, O. Palamutçuogullari, and S. B. Yarman, "3.5-3.8 GHz class-E balanced GaN HEMT power amplifier with 20 W Pout and 80% PAE," *IEICE Electron. Exp.*, vol. 10, no. 5, p. 20130104, 2013.
[8] J. Kim *et al.*, "6–18 GHz, 26 W GaN HEMT compact power-combined non-uniform distributed amplifier," *Electron. Lett.*, vol. 52, no. 25, pp. 2040–2042, Aug. 2016.
[9] H. Wang, B. Tang, Y. Wu, C. Yu, and Y. Liu, "A novel dual-band balanced power amplifier using branch-line couplers with four arbitrary terminated resistances," *Prog. Electromagn. Res. C*, vol. 60, no. 5, pp. 67–74, 2015.
[10] Cree. *10-W RF Power GaN HEMT (CGH40010)*. Accessed: Nov. 2, 2017. [Online]. Available: http://www.wolfspeed.com/cgh40010
[11] P. Colantonio, F. Giannini, E. Limiti, and V. Teppati, "An approach to harmonic load- and source-pull measurements for high-efficiency PA design," *IEEE Trans. Microw. Theory Techn.*, vol. 52, no. 1, pp. 191–198, Jan. 2004.
[12] L. M. George, Y. Leo, and E. Jones, *Microwave Filters, Impedance-Matching Networks, and Coupling Structures*. Norwood, MA, USA: Artech House, 1980, pp. 434–497.
[13] P. I. Richards, "Resistor-transmission-line circuits," *Proc. IRE*, vol. 36, no. 2, pp. 217–220, Feb. 1948.
[14] K. Kuroda, "General properties and synthesis of transmission-line networks," in *Microwave Filters and Circuits*, vol. 22. A. Matsumoto, Ed. New York, NY, USA: Academic, 1970.
[15] K. Niotaki, A. Collado, A. Georgiadis, and J. Vardakas, "5 watt GaN HEMT power amplifier for LTE," *Radioengineering*, vol. 23, no. 1, p. 339, 2014.

WAQAR AHMAD MALIK received the B.S. degree in electrical engineering from the NWFP University of Engineering and Technology, Peshawar, Pakistan, in 2004, and the M.S. degree in radio systems engineering from The University of Hull, U.K., in 2006. He joined academia as a Lecturer and taught for a total of five years at the University of Engineering and Technology, Mardan Campus, Pakistan, and the National University of Computer and Emerging Sciences, Peshawar Campus, Pakistan.

He is currently pursuing the Ph.D. degree with the Electrical Engineering Department, King Saud University, Riyadh, Saudi Arabia. His research interest includes optimization of microwave circuits, broadband matching circuits, and device modeling, computer-aided circuit design, and wideband high-power amplifiers.

ABDELFATTAH AHMAD SHETA received the degree from the Faculty of Engineering, Alexandria University, Egypt, in 1985, the M.Sc. degree in electrical engineering from Cairo University, Egypt, in 1991, and the Ph.D. degree in microwave circuits analysis and design from ENST, Université de Bretagne Occidentale, France, in 1996.

He is currently a Full Professor with the Electrical Engineering Department, King Saud University, Riyadh, Saudi Arabia. His current research interests include reconfigurable RF system, UWB systems, microstrip antennas, antennas for hyperthermia applications, microstrip filters, planar and uniplanar MICs and MMICs, and high-efficiency power amplifiers.

IBRAHIM ELSHAFIEY received the B.S. degree in communications and electronics engineering from Cairo University in 1985, and the M.S. and Ph.D. degrees from Iowa State University in 1992 and 1994, respectively. He is currently a Professor with the Electrical Engineering Department, King Saud University. His research interests include computational electromagnetics, biomedical imaging, communication systems, and nondestructive evaluation.